



UNIVERSITY OF LEEDS

This is a repository copy of *Explosion Flame Acceleration over Obstacles: Effects of Separation Distance for a Range of Scales*.

White Rose Research Online URL for this paper:  
<http://eprints.whiterose.ac.uk/111835/>

Version: Accepted Version

---

**Article:**

Na'inna, AM, Phylaktou, HN [orcid.org/0000-0001-9554-4171](http://orcid.org/0000-0001-9554-4171) and Andrews, GE [orcid.org/0000-0002-8398-1363](http://orcid.org/0000-0002-8398-1363) (2017) Explosion Flame Acceleration over Obstacles: Effects of Separation Distance for a Range of Scales. *Process Safety and Environmental Protection*, 107. pp. 309-316. ISSN 0957-5820

<https://doi.org/10.1016/j.psep.2017.01.019>

---

© 2017 Published by Elsevier B.V. on behalf of Institution of Chemical Engineers. This is an author produced version of a paper published in *Process Safety and Environmental Protection*. Uploaded in accordance with the publisher's self-archiving policy.

**Reuse**

Items deposited in White Rose Research Online are protected by copyright, with all rights reserved unless indicated otherwise. They may be downloaded and/or printed for private study, or other acts as permitted by national copyright laws. The publisher or other rights holders may allow further reproduction and re-use of the full text version. This is indicated by the licence information on the White Rose Research Online record for the item.

**Takedown**

If you consider content in White Rose Research Online to be in breach of UK law, please notify us by emailing [eprints@whiterose.ac.uk](mailto:eprints@whiterose.ac.uk) including the URL of the record and the reason for the withdrawal request.



[eprints@whiterose.ac.uk](mailto:eprints@whiterose.ac.uk)  
<https://eprints.whiterose.ac.uk/>

## Accepted Manuscript

Title: Explosion Flame Acceleration over Obstacles: Effects of Separation Distance for a Range of Scales

Authors: A.M. Na'inna, H.N. Phylaktou, G.E. Andrews

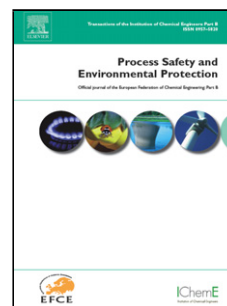
PII: S0957-5820(17)30024-1  
DOI: <http://dx.doi.org/doi:10.1016/j.psep.2017.01.019>  
Reference: PSEP 959

To appear in: *Process Safety and Environment Protection*

Received date: 5-9-2016  
Revised date: 14-1-2017  
Accepted date: 22-1-2017

Please cite this article as: Na'inna, A.M., Phylaktou, H.N., Andrews, G.E., Explosion Flame Acceleration over Obstacles: Effects of Separation Distance for a Range of Scales. *Process Safety and Environment Protection* <http://dx.doi.org/10.1016/j.psep.2017.01.019>

This is a PDF file of an unedited manuscript that has been accepted for publication. As a service to our customers we are providing this early version of the manuscript. The manuscript will undergo copyediting, typesetting, and review of the resulting proof before it is published in its final form. Please note that during the production process errors may be discovered which could affect the content, and all legal disclaimers that apply to the journal pertain.



# Explosion Flame Acceleration over Obstacles: Effects of Separation Distance for a Range of Scales

A.M. Na'inna<sup>a\*</sup>, H.N. Phylaktou<sup>b</sup>, and G.E. Andrews<sup>b</sup>

<sup>a</sup>Armament Engineering Department, Nigerian Air Force Institute of Technology, Kaduna, Nigeria

<sup>b</sup>Energy Research Institute, University of Leeds, Leeds, United Kingdom, LS2 9JT

\* Corresponding Author. Tel: +2348030679898

Email address: abdulmajid.nainna@airforce.mil.ng; amnainna@gmail.com

## HIGHLIGHTS

1. A dependence of overpressure and flame speed on the obstacle scale agrees with a square relationship between them.
2. The maximum overpressure and flame speed increased with reduction in number of flat-bars.
3. The worst case obstacle spacing increase with increase in obstacle scale.
4. The average value of  $S_T/S_L$  obtained is similar to that from the analysis of some real gas explosion incidents.

## Abstract

The influence of obstacle separation distance on explosion flame acceleration was studied for 10% methane-air mixtures using two 20% blockage obstacles with variable number and width of bars (variable obstacle length scale) were investigated in a 162 mm diameter 4.5 m long tube with ignition on the centre of the closed end and flame propagation towards the open end. The spacing between the obstacles was varied from 0.25 m to 2.75 m. It was observed that the maximum overpressure and flame speed increased with the reduction in number of flat-bars (i.e. with increasing obstacle length scale). A maximum overpressure of 129 kPa at 2.25 m obstacle spacing was achieved with 1-flat-bar obstacles, followed by 118 kPa and 110 kPa for 2 and 4-flat-bars respectively at 1.25 m and 0.5 m obstacle separation. Turbulent to laminar burning velocity ratios

---

downstream of the second obstacle at the optimum spacing for maximum interaction were in the range of 62-122. These are the magnitudes of flame acceleration required to explain overpressures in vapour cloud explosions in the presence of obstacles. It is worth appreciating that two obstacles of lower blockages but spaced optimally could generate higher explosion severity in terms of overpressure, flame speed and turbulence level similar to real gas explosion incidents.

*Keywords:* Explosions; flame acceleration; obstacle separation distance; obstacle scale; turbulent flames.

### Nomenclature

b (m)	obstacle scale	P (kPa)	explosion overpressure
BR (-)	obstacle blockage ratio	$R_\ell$ (-)	turbulent Reynolds number
D (m)	obstacle tube diameter	$S_f$ (m/s)	flame speed
$D_{\text{tube}}$ (m)	explosion tube diameter	$S_g$ (m/s)	unburned gas velocity
K (-)	pressure loss coefficient	$S_L$ (m/s)	laminar burning velocity
$K_a$ (-)	Karlovitz number	$S_T$ (m/s)	turbulent burning velocity
L (m)	length of explosion tube	$u'$ (m/s)	root mean square velocity
$Le$ (-)	Lewis number	$\nu$ (m <sup>2</sup> /s)	kinematic viscosity
$\ell$ (m)	integral length scale	x (m)	distance downstream of an obstacle
n (-)	number of rows of obstacles	$x_s$ (m)	obstacle separation distance

## 1. Introduction

The spacing between obstacles is one of the main factors that influence the severity of gas explosions in congested medium. However, despite previous studies on obstacle spacing, there is still need for more systematic study of this important factor. On one side, obstacles closely separated to each other give no space for the development of the jet shear layers that generate turbulence[1]. On the other side, obstacles that are widely spaced allow the turbulence generated downstream of the first obstacle to decay thereby slowing down the flame speed before reaching the second obstacle and there is reduced or no interaction[1]. In between the widely spaced and closely spaced obstacles, there has to be a spacing that would produce worst case explosion interaction. In the literature, highly congested enclosures have been studied, often with geometries that have obstacles too close to generate the worst case interaction, hence not complying with the ATEX directive[2]. The ATEX directive

requires the worst case explosion scenarios or highest risk to be assessed for the severity of the hazard posed by gas explosions in process plants or on offshore oil and gas platforms [2]. In order to avoid maximum overpressure in plant design, it is necessary to avoid optimum spacing between obstacles and to do this, design information is needed on the worst case obstacle separation.

As part of a wider assessment of the effects of obstacles on gas explosions, a number of experimental studies have established a strong influence of obstacle separation distance [3-13]. In most cases many repeat obstacles were spaced closely ranging from 1.3 to 10 obstacle scales,  $b$ .

One of the most wide-ranging investigations of explosion accelerations in congested volumes was in the MERGE programme [14]. Gardner *et al.* [15] analysed this data and showed that the overpressure for all the geometries investigated could be correlated by Eq. 1.

$$P_{\max} = 4.8 \times 10^{-4} n^3 BR^2 D^{0.7} S_L^3 \quad (1)$$

where  $n$  is the number of rows of obstacles (varied from 8 to 30).

$BR$  is the blockage area ratio (varied from 0.265 – 0.521).

$D$  is the obstacle tube diameter, which is proportional to the obstacle length scale,  $b$  (varied from 19 – 168 mm).

$S_L$  is the laminar burning velocity (varied from 0.4 – 1.35 m/s).

Missing from this correlation and from the experimental work is the influence of the obstacle separation, which was investigated in the present work. In congested but unconfined explosions the peak overpressure,  $P_{\max}$ , is approximately proportional to the square of the flame speed and from Eq. 1 the flame speed would scale linearly with  $BR$  and  $D^{0.35}$ . The flame speed is linked to the turbulent burning velocity by the combustion expansion ratio,  $E$  and as this is fixed for a mixture composition. The turbulent burning velocity from Eq. 1 is expected to vary linearly with the blockage ratio and with the length scale, which is proportional to  $D$ . Equation. 1 shows the importance of repeated

obstacles with a cubic dependence on the overpressure. However, the relatively large dependence on the  $D$  could be an indirect effect of the separation distance not being included in the correlation. In the MERGE data the separation distance was not systematically varied and the relative separation distance  $x_s/D$  was not held constant as  $D$  was varied. Thus the role of  $D$  could have included some effect of separation distance.

Gardner *et al.* [15] used a test rig similar to the present equipment to investigate how the obstacle length scale,  $b$  influences the flame acceleration in explosions with a single 30% blockage ratio. The authors showed that the downstream flame speed is enhanced as the length scale was increased, with maximum flame speeds of 250 m/s for the highest length scale investigated of 38.5mm, which is at the lower value of the range examined in the MERGE programme [14]. The highest length scale and the peak overpressure in the work of Gardner *et al.* [15] occurred at 21 length scales downstream of the obstacle. Gardner *et al.* [15] established a dependence of the overpressure on  $b$  at a maximum of  $b^{0.25}$ , which is less than the 0.35 exponent that arises from the MERGE data in Eq. 1.

Phylaktou and Andrews [16] studied the influence of flame acceleration over a single obstacle with a single hole, in a 76 mm tube diameter and 2 m long tube explosion with the blockage ranging from 20 to 80%. Figure 1 shows a schematic diagram for the 20% and 80% single-hole obstacles used by the authors.

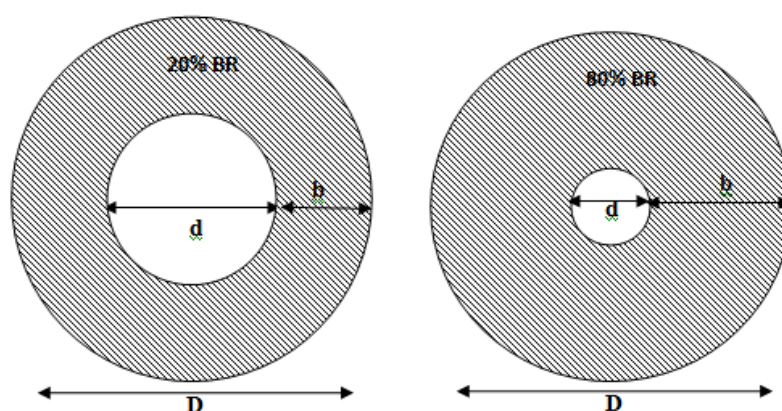


Fig. 1. Schematic diagram of 20% and 80% obstacle blockage ratio (BR) used by Phylaktou and Andrews [16].

Using an explosion induced unburned mean gas velocity flow,  $S_g$  of 29 m/s upstream of the obstacles, it was shown that the peak flame speed varied linearly with the BR, as predicted by Eq.1. The authors also showed that the maximum flame speed occurred at 7 tube diameters behind the obstacle for a BR of 40% to 80% and 3 and 4 diameters downstream for a BR of 20% and 30%. Table 1 shows a summary of positions to maximum flame speeds for single obstacle tests in the literatures. The obstacle scale,  $b$  for a given blockage was calculated using Eq. 2 as:

$$b = D_{\text{tube}} - 0.95d_{\text{hole}} \quad (2)$$

These distances are similar to those found by Gardner *et al.* [15] with  $x/b=21$  for a 30% BR. These are relatively large distances corresponding to a large number of turbulent length scales.

Table 1. Position to maximum flame speed from single obstacle tests in the literatures.

References (-)	$D_{\text{tube}}$ (m)	$d_{\text{hole}}$ (m)	$L_{\text{tube}}$ (m)	BR (%)	$b$ (m)	$x/b$ (-)
Gardner et al. [15]	0.162	0.136	4	30	0.033	21
Phylaktou and Andrews [16]	0.076	0.068	2	20	0.011	28
Phylaktou and Andrews [16]	0.076	0.064	2	30	0.016	21
Phylaktou and Andrews [16]	0.076	0.059	2	40	0.020	31
Phylaktou and Andrews [16]	0.076	0.034	2	80	0.044	19

Generally, for the highest flame acceleration between two successive obstacles to occur, the second obstacle would have to be at the location just downstream of where the peak flame speed behind the first obstacle occurred. If the spacing is wider, the flame speed downstream of the first obstacle would be decelerating before reaching the second obstacle and if shorter the flame would still be accelerating, before interacting with the second obstacle. In both cases, the flame acceleration downstream of the second obstacle would not be as high as when the two obstacles are optimally spaced.

Na'inna et al. [17] reported an experimental study in an elongated tube with two orifice plate obstacles of 30% BR each and 10% methane/air as explosible mixture. The spacing between the double obstacles was systematically varied from 0.5 m to 2.75 m. A clear effect of obstacle

separation distance on gas explosion severity (flame speed and overpressure) was established with an obstacle separation of 1.75 m which produced close to 300 kPa overpressure and a flame speed of 500 m/s. These values were higher by a factor of two when compared to the overpressure and flame speed with an obstacle separation distance of 2.75 m. Na'inna et al. [17] also showed that there is an agreement between the dependence of maximum explosion severity on the separation distance and turbulence profile determined in cold flow by other researchers. Nonetheless, the results showed that the peak acceleration of the flame emerged further downstream of the obstacle than the position of maximum turbulence determined in the cold flow studies.

Na'inna et al. [18] have also examined the effect of mixture reactivity on the optimum obstacle spacing for two single-hole obstacles of 30% blockage ratio with variable obstacle separation distance. A flame speed of over 1 km/s, i.e. close to detonation, was reached for 4.5% propane/air mixtures with two obstacles optimally spaced. Furthermore, leaner mixtures of 7% methane/air and 3% propane/air mixtures were investigated and flame speeds of 280 m/s were measured. This shows that severe flame acceleration can occur with comparatively uncongested geometries of low BR and optimally spaced obstacles.

In furtherance to the study of effects of obstacle separation distance on gas explosions, Na'inna et al. [19] investigated the influence of obstacle blockage ratio. A series explosion tests were performed using methane-air (10% by vol.), in an elongated vented cylindrical vessel 162 mm internal diameter with an overall length-to-diameter,  $L/D$  of 27.7. Double 20-40% blockage ratio orifice plates with their spacing varied systematically from 0.5 m to 2.75 m were used as obstacles. The 40% BR produced the highest explosion severity in terms of overpressure and flame speeds which is 340 kPa and 716 m/s respectively when compared to 30% BR (270 kPa and 486 m/s) and 20% BR (120 kPa and 362 m/s). This shows that the explosion severity increased with increase in obstacle blockage ratio. However, the worst case obstacle spacing was found to be shorter with increase in obstacle blockage. The worst case spacing were 35, 53 and 94 obstacle scales for 40%, 30% and 20% obstacle blockage ratios respectively.

The present work studied the interaction of two obstacles having a BR of 20% with the aim of focusing on the effect of the obstacle characteristic scale. To this purpose, flat bar obstacles were used as these had a more easily defined and uniform length scale, compared to circular hole grid plates.

## 2. Experimental

The explosion tests were conducted indoors to prevent adverse weather effects on the results, save cost, protect the environment from pollution and to carry out small scale tests. Prior to any test, the ambient temperature, pressure and humidity were all recorded.

The main test vessel, shown in Fig. 2, was a 162 mm internal diameter tube with a total length of 4.25m corresponding to a length-to-diameter ratio,  $L/D_{\text{tube}}$ , of 27.7. The explosion tube was constructed from eight flanged sections, each 0.5 m long, and one section 0.25 m long.

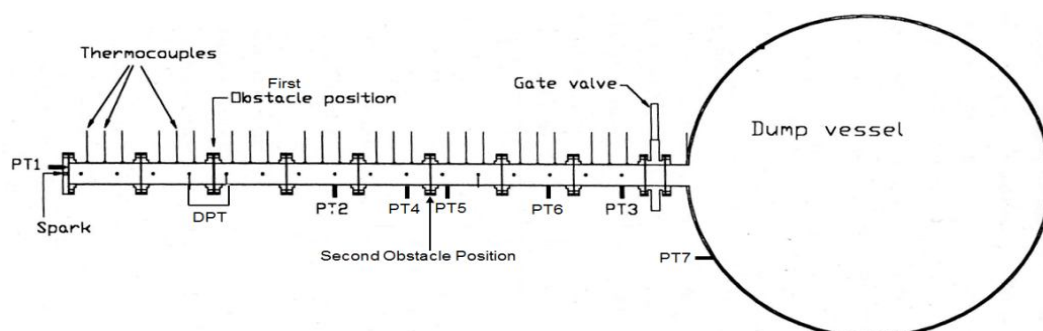


Fig. 2. A schematic diagram of the experimental set-up.

The spacing between the obstacles could be varied in 0.25m increments by moving the position of the 0.25m long section. The test vessel was designed and tested to withstand overpressures of 3,500 kPa so that a detonation could occur safely. The horizontally mounted explosion tube was closed at the ignition end, while its open end connected to a 50m<sup>3</sup> cylindrical dump-vessel which contained the very fast flame emerging from the test rig.

Figure 3 shows the flat-bar obstacles that were used, made from stainless steel of 3.2 mm thick. All the obstacles investigated had 20% blockage. The integral length scale,  $\ell$ , was proportional to (and of

the order of) the obstacle width of the bar,  $b$ . The first obstacle was fixed at 1 m downstream of the spark for all tests thereby giving an upstream explosion section of  $L/D_{\text{tube}}$  of 6.2.



Fig. 3. Obstacles used in the current research: 1-4 flat bar of 20% blockage ratio each.

In the section up to the first obstacle, a laminar flame accelerates due to preferential expansion axially thus resulting in upstream flame speed of 25 m/s upon approaching the first obstacle. This corresponds to unburned gas velocities ahead of the flame of typically 86% of the laminar flame speed for 10% methane/air [16]. A pneumatically actuated gate valve isolated the test vessel from the dump vessel prior to mixture preparation, allowing evacuation of the test vessel and mixture preparation using partial pressures. A stoichiometric mixture of methane in air (10% by vol.) was used in all the tests in this work. After mixture circulation using a recirculation pump for at least 4 volume changes, the gate valve was opened and a 16 Joule spark plug ignition was initiated at the centre of the test vessel ignition-end flange.

An array of 24 type-K mineral insulated exposed junction thermocouples, positioned along the axial centre line of the explosion tube were used to record the time of flame arrival and thus flame speeds. The exposed thermocouple bead ensured an immediate response. The large thermal mass ensured that the thermocouple did not measure the true burnt gas temperature and hence melt; the aim was not to examine the temperature but rather to detect the change in temperature due to the flame arrival. The test vessel and dump vessel pressure histories were measured using 8 Keller-type piezo-resistive pressure transducers located as shown in Fig. 2. The unburned gas velocity ahead of the flame was determined by using the obstacle as an orifice plate flow meter with the wall static pressure measured at  $1D_{\text{tube}}$  upstream and  $0.5D_{\text{tube}}$  downstream of the first obstacle giving the differential pressure across the obstacle. For the measurement of gas flow induced velocity ahead of

the accelerating flame through the second obstacle, pressure transducers PT4 and PT5 positioned at  $1D_{\text{tube}}$  upstream and  $0.5D_{\text{tube}}$  downstream of the second obstacle were used. From the obtained unburned gas flow velocity measurements, the turbulence downstream of the obstacles could be estimated based on the obstacles overall pressure loss, as detailed later.

A 32-channel (maximum sampling rate of 200 kHz per channel) transient data recorder (Data Logger and FAMOS software) was used to record and process the data. Each test was performed thrice so as to demonstrate repeatability and ensure representative data and the average of the repeat tests was used for the analysis of the flame speed and overpressure. Table 2 shows a summary of the tests carried out and their corresponding results.

Table 2. Summary of test conditions and results.

Test	$N_{\text{obst}}$	$N_b$	$x_s$	$b$	$\ell$	$S_g$	$S_{\text{fmax}}$	$P_{\text{max}}$	$u'/S_L$	$R_\ell$	$S_{T\text{max}}/S_L$	Ka
(-)	(-)	(-)	(m)	(m)	(m)	(m/s)	(m/s)	(kPa)	(-)	(-)	(-)	(-)
1	-	-	-	-	-	-	122	26	-	-	-	-
2	1	1	-	0.026	0.013	55	240	67	14	5314	71	0.43
3	2	1	1.75	0.026	0.013	89	360	115	23	11024	107	0.77
4	2	1	2.25	0.026	0.013	118	412	129	30	14722	122	1.18
5	2	1	2.75	0.026	0.013	111	281	81	28	12893	84	1.11
6	1	2	-	0.013	0.006	49	227	56	12	2464	67	0.49
7	2	2	1	0.013	0.006	92	333	98	24	6086	98	1.12
8	2	2	1.25	0.013	0.006	91	386	118	23	6127	116	1.07
9	2	2	2.25	0.013	0.006	95	360	108	24	5824	107	1.21
10	1	4	-	0.006	0.003	45	206	43	11	1108	62	0.61
11	2	4	0.25	0.006	0.003	58	276	97	15	1965	82	0.78
12	2	4	0.5	0.006	0.003	56	356	110	14	1785	107	0.76
13	2	4	1	0.006	0.003	79	348	77	20	2348	102	1.31

$N_{\text{obst}}$  = Number of obstacle;  $N_b$  = Number of flat bar;  $x_s$  = obstacle separation distance;  $b$  = obstacle length scale;  $S_g$  = explosion induced gas velocity;  $S_{\text{fmax}}$  = maximum flame speed;  $P_{\text{max}}$  = maximum explosion overpressure;  $u'/S_L$  = ratio of root mean square velocity to laminar burning velocity;  $R_\ell$  = turbulent Reynolds number;  $S_{T\text{max}}/S_L$  = ratio of maximum turbulent flame speed to laminar burning velocity; Ka = Karlovitz number

### 3. Results and discussion

#### 3.1 Explosion overpressure and flame speed

Figure 4 shows the influence of the maximum overpressure and flame speed for single obstacles on obstacle scale,  $b$  for all the flat-bar obstacles.  $P_{\text{max}}$  scales with  $b^{0.33}$  and the flame speed scales with  $b^{0.15}$  and this agrees with a roughly square relationship between overpressure and flame speed. These are similar to the dependencies previously found [20-22]. However, the length scale exponents are

less than those from the MERGE experiment as given in Eq.1, but are similar to those that arise from turbulent burning velocity considerations [20-22].

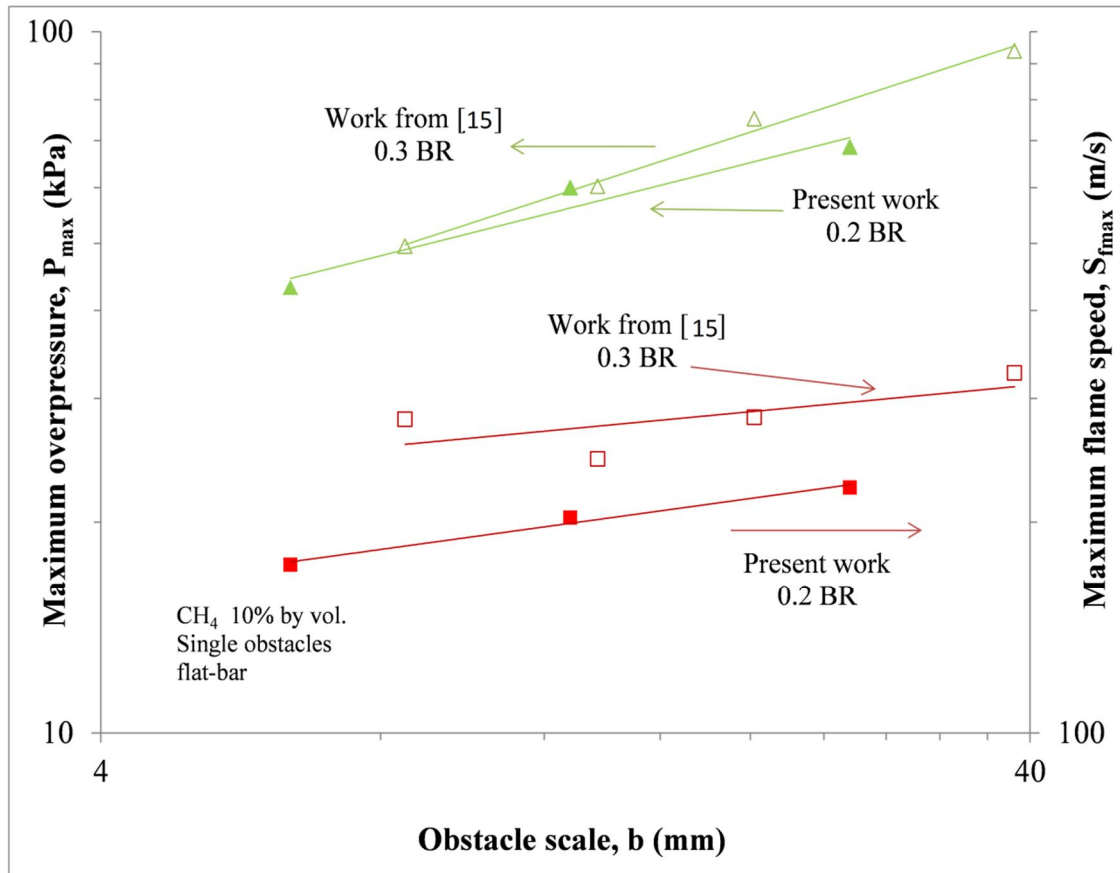


Fig. 4. Relationship between maximum overpressures and flame speeds against obstacle scale for single obstacles of 1-4 flat-bars.

The pressures measured with PT3 as a function of time are shown in Fig. 5, for three different obstacle separation distances with the 1-flat-bar obstacles. An influence of obstacle spacing was discernible in terms of the maximum pressure as well as the profile of the pressure development. From the point of ignition up to the point of flame interaction with the first obstacles (at around 67ms), the pressure and flame development was very similar in the three cases. For all the obstacle separation distances, there was sudden rise in overpressure downstream of the first obstacle with the peak overpressures for the first obstacle taking place at nearly the same time.

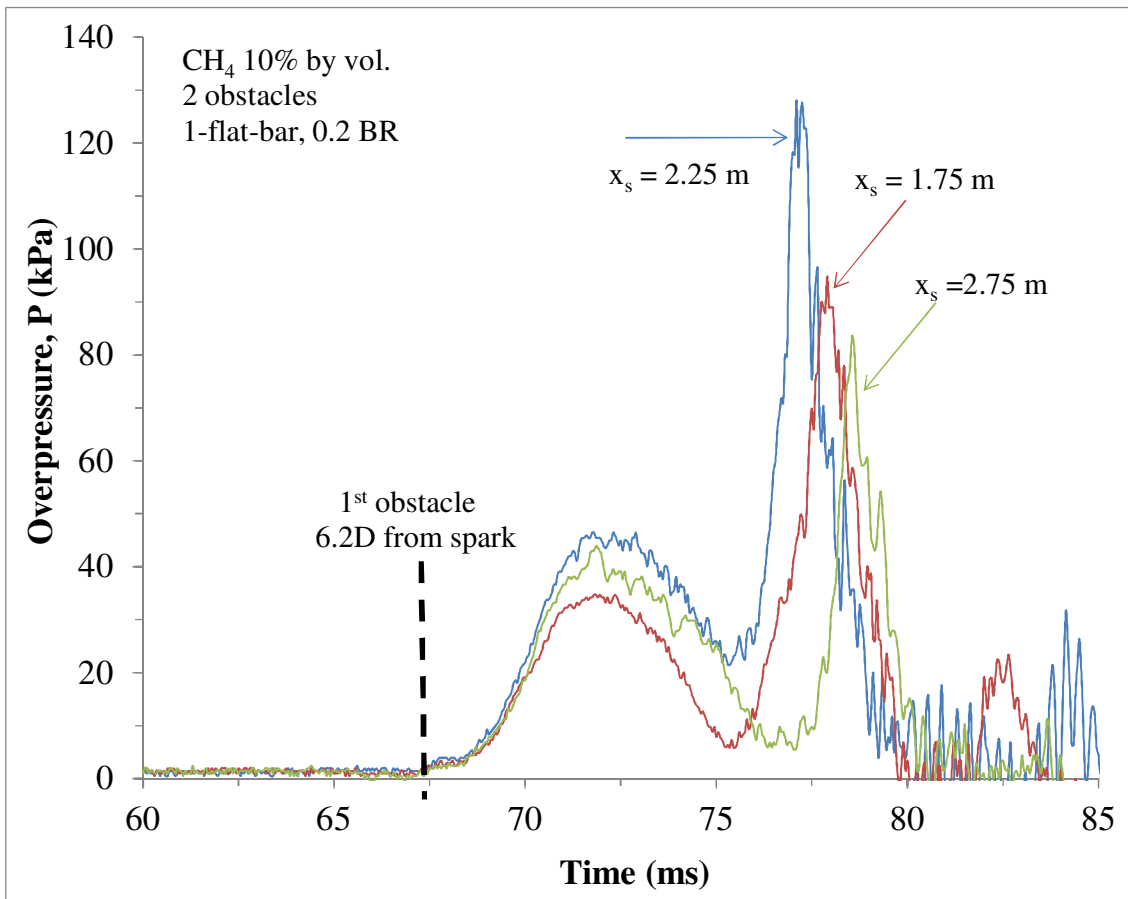


Fig. 5. Pressure-time records for double 1-flat-bar obstacles at different obstacle separation distances.

The maximum interaction effect of the double obstacles was attained at an obstacle spacing of 2.25m where the flame accelerated to its highest value after the first obstacle before getting to the second. This in turn induced the maximum unburnt gas velocities through the second obstacle thereby resulting in the peak turbulence downstream and thus highest flame speeds and overpressures when the flame reached this region. This behaviour is similar to the non-reacting flow turbulence-intensity profile behind a grid plate [23].

Figure 6 presents the maximum overpressure as a function of the dimensionless obstacle spacing,  $x_s/b$ , for 1-4 flat-bar obstacles. Also shown is the intensity of turbulence against dimensionless distance downstream of a bar-grid obstacle of 0.22 BR [23]. The peak overpressure increased with the reduction in number of flat-bars, which decreased the obstacle scale,  $b$ . A maximum overpressure of 129 kPa at 2.25 m obstacle spacing was found with 1-flat-bar obstacle followed by 118 kPa bar and 110 kPa for 2 and 4-flat-bars respectively at 1.25 m and 0.5 m obstacle separation.

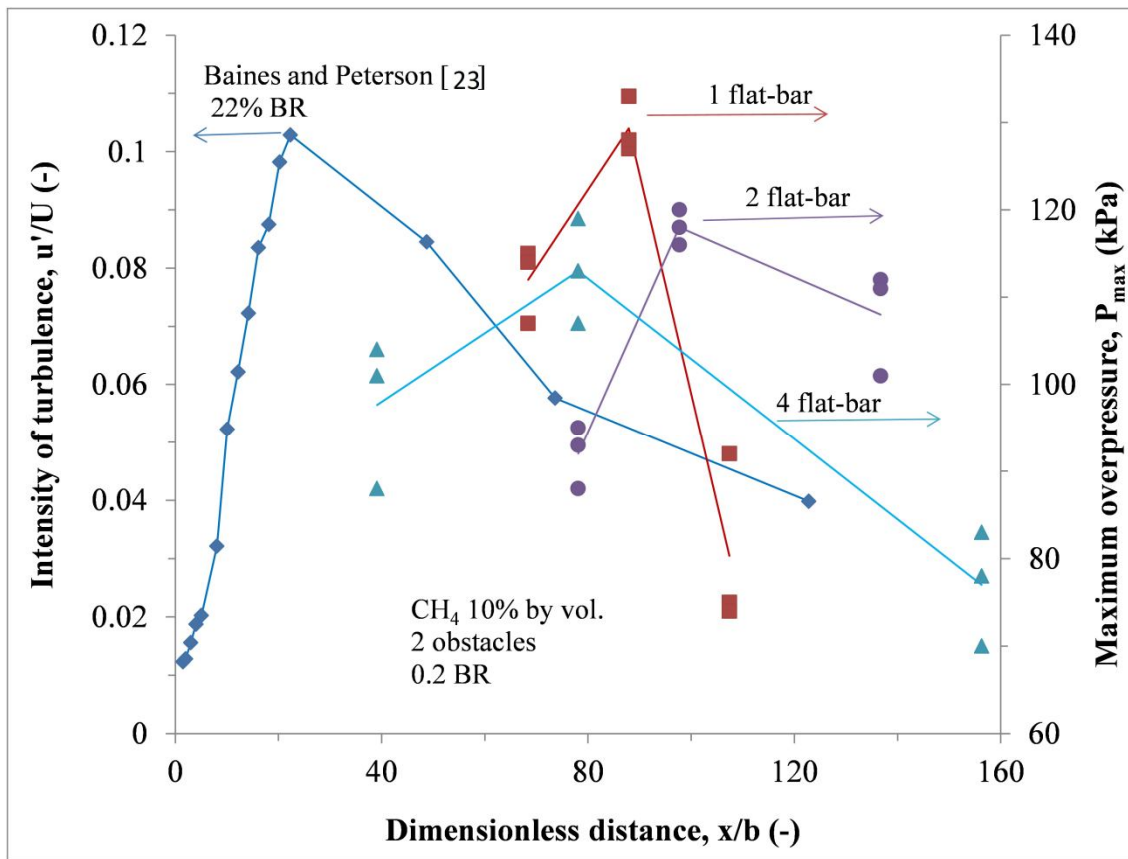


Fig. 6. Comparison between intensity of turbulence from cold flow turbulence [23] and transient experimental work with flat-bar obstacles.

The optimum obstacle spacing for the worst case overpressure for all the obstacles demonstrated a related axial variation of overpressure to that of maximum turbulence intensity from non-reacting turbulent flow studies [23]. However, for similar obstacle blockage ratio (0.2 BR) the cold flow turbulence achieved its highest value closer to the obstacle than for the peak overpressure. This could be attributed to turbulence convection downstream by the mean unburned gas velocity once the flame has passed through the first obstacle in transient explosions. The highest flame speeds as a function of the dimensionless obstacle spacing are shown in Fig. 7. The dependence of obstacle scale and obstacle spacing on the peak flame speeds were similar to those for the maximum overpressures.

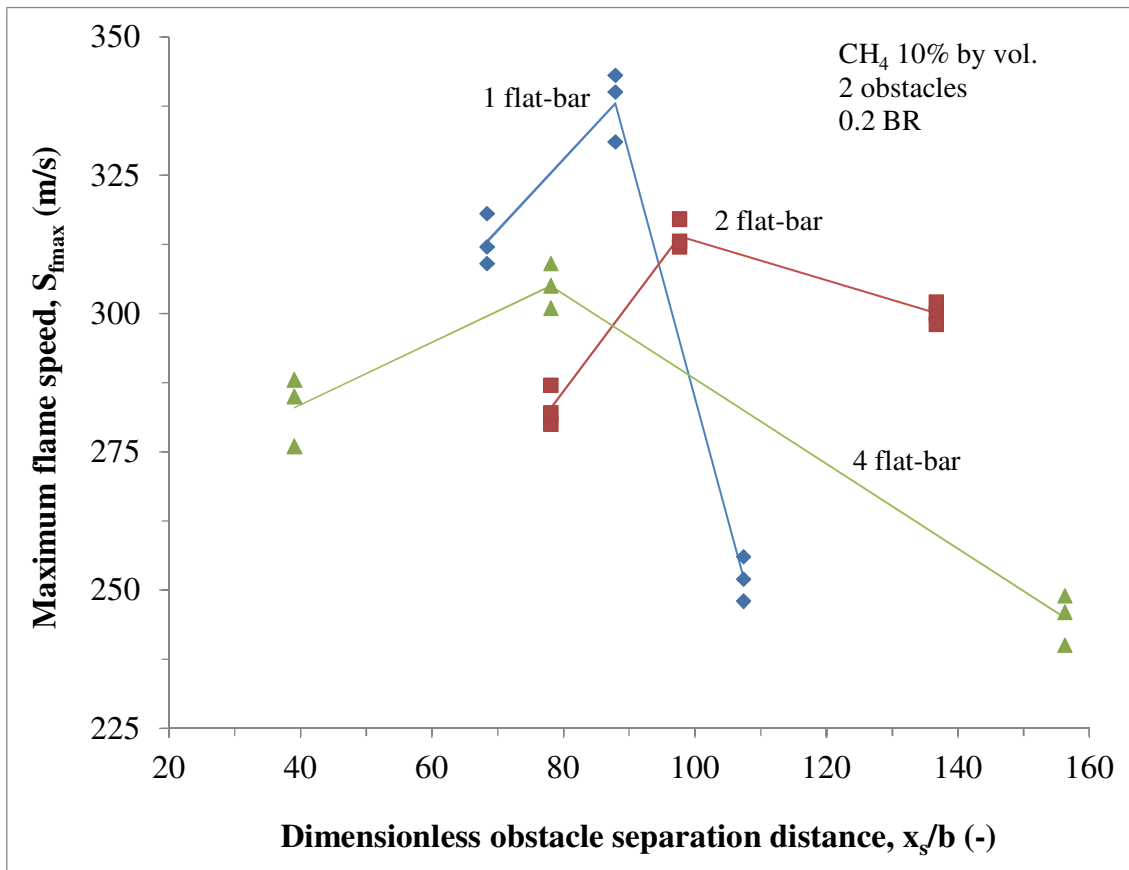


Fig. 7. Influence of obstacle scale on maximum flame speeds (showing all repeat tests) and dimensionless obstacle spacing.

### 3.2 Turbulent burning velocity as a function of the predicted peak turbulence, $u'$ .

In this section the explosion test data are presented in terms of fundamental turbulent combustion parameters which allow the comparison to other data and combustion models in the literature and thus widens the usefulness and applicability of the work.

Using data from cold flow turbulence tests [23, 24] induced by grid plates, Phylaktou and Andrews [24] predicted the maximum turbulence intensity where the highest explosion severity transpires. It is assumed that the highest burning velocity behind an obstacle takes place at the peak turbulence location. These data give  $u'/S_g$  as a function of the dimensionless distance,  $x$  from the grid plate divided by the obstacle scale,  $b$ . In order to evaluate the turbulent mean fluctuating velocity  $u'$ , the upstream induced unburned gas flow velocity,  $S_g$ , needs to be known. In the present work, the  $S_g$  was measured by using the obstacle as an orifice plate flow meter [25]. At a prevailing temperature, the

$S_g$  is thus given as the ratio of mass flow rate to the area of the 162 mm diameter tube and by the upstream gas density, evaluated at the static pressure upstream.

Phylaktou and Andrews [24] have indicated that published data [23] for the maximum turbulence intensity behind sharp edged grid plate type obstacles, as used in the present work, is given by Eq. 3.

$$u'/S_g = 0.225\sqrt{K} \quad (3)$$

The pressure loss coefficient of the obstacle,  $K$ , was obtained from the correlation of Ward Smith [26] data. The calculated values of  $u'$  for a given mean flow velocity,  $S_g$ , was used to determine the maximum turbulent Reynolds number,  $R_\ell$  in Eq. 4.

$$R_\ell = \frac{u' \ell}{\nu} \quad (4)$$

Where  $\nu$  is the kinematic viscosity is whereas  $\ell$  is the integral length-scale which is determined by the physical dimensions of the obstacle. The integral length scale was taken to be half of the obstacle scale,  $b$  [23, 24]. The  $R_\ell$  at the point of peak intensity turbulence behind the obstacles used in the present work are given in Table 2.

The measured flame speed,  $S_f$ , is the product of the adiabatic expansion ratio,  $E$  (which is 8 for 10% methane-air mixtures), and the turbulent burning velocity,  $S_T$ . The turbulent burning velocities were obtained from the measured maximum  $S_f$ . The variation in the  $S_{Tmax}/S_L$  in Table 2 was from 62 to 122 which is corresponding to  $S_{Tmax}$  of 28 to 55 (with  $S_L = 0.45$  m/s). These numbers are used to measure the level of turbulence in gas explosions. The current range of  $S_{Tmax}/S_L$  indicates high turbulence level generated. Interestingly, even some real gas explosions incidents with high level of congestion had their  $S_T/S_L$  within the range obtained in present work [15,16] with just two low blockage obstacles optimally separated.

An attribute of a highly turbulent flame is local flame quenching due to a high turbulence which over-stretch the flame [21, 27]. The flame straining is given as the Karlovitz stretch factor otherwise

known as the Karlovitz number,  $Ka$ , which is defined as the ratio of the chemical lifetime of the combustion process,  $\tau_c$  to the turbulent lifetime,  $\tau_\ell$ . The relationship between  $Ka$  and turbulent Reynolds number,  $R_\ell$  was established by Abdel-Gayed *et al.* [28] and shown in Eq. 5.

$$Ka = 0.157 \left( \frac{u'}{S_L} \right)^2 R_\ell^{-0.5} \quad (5)$$

At high turbulence levels, partial or full flame quenching could occur due to flame front fragmentation [28,29]. For non-isotropic turbulence generated downstream of a grid plate, up to and after the position of maximum turbulence where the flame velocity is at its peak, full flame quenching was never observed. However, for isotropic turbulence, full flame quenching is observed. Phylaktou and Andrews [16] proved that in single grid plate explosions there could be partial but not complete flame quenching even in regions where  $KaLe$  was  $>1.5$ , which was the flame extinction limit reported by Abdel-Gayed *et al.* [28] in their fan-stirred turbulent closed vessel explosion experiments. The Lewis number ( $Le$ ) is nearly unity for a stoichiometric methane-air mixture, and therefore flame quenching would be anticipated based on the Abdel-Gayed *et al.* [28] criteria for values of  $Ka$  greater than 1.5. Table 2 shows that in the present work the maximum  $Ka$  at the peak flame speed was 1.31 and so no quenching would be expected. Abdel-Gayed *et al.* [30] presented another correlation of flame quenching for  $Ka \geq 1$ . Further examinations on flame extinction were conducted by Bradley *et al.* [31]. The authors showed that  $KaLe > 1.5$  corresponded to the lower boundary of the quenching process and a new quench limit was established to be  $KaLe \geq 6$  [31]. This therefore shows that turbulent flame quenching would not take place in multi-obstacle explosions unless the turbulence levels were high enough to achieve close to detonation conditions. In the present work with turbulent to laminar burning velocity ratios up to 120, no total flame quench was observed.

Figure 8 shows a plot of turbulent to laminar burning velocity ratios as a function of  $u'/S_L$  and compared with the correlation of Bradley *et al.* [31]. Also included in Fig. 8 are the previous results of Na'inna *et al.* [17,18] for orifice plate circular hole grid plates of 30% BR with varying separation

distance and for different mixture reactivities. Figure 8 also includes the data range from the review of turbulent to laminar burning velocity ratio of Phylaktou *et al.* [32,33], which extends to  $S_T/S_L$  of 120. The mean line through this experimental data was fitted using Eq. 6.

$$S_T/S_L = 1 + C u'/S_L \quad (6)$$

where  $C$  is a constant that has a value of 2 for the mean of the data range in the literature, but varies between 4 and 0.5 to include most of the data. The value of 2 is typical of data for hydrocarbon fuels and lower values are more typical of hydrogen. The correlation of Abdel-Gayed *et al.* [29] can be expressed in the form of Eq. 6, when  $C$  becomes  $0.88/(KaLe)^{0.3}$ . For  $KaLe$  values ranging from 10 to 0.01,  $C$  varies from 0.4 to 3.5 and these values are similar to the range obtained from the experimental data.  $C$  is  $< 2$  if  $Ka$  is high, which occurs if  $S_L$ ,  $R_\ell$  or  $u'$  is high, such as for hydrogen or large turbulent length scales. Conversely  $C$  is  $> 2$  if  $Ka$  is low, which occurs if  $S_L$ ,  $R_\ell$  or  $u'$  is low such as for lean methane mixtures or for small turbulent length scales.

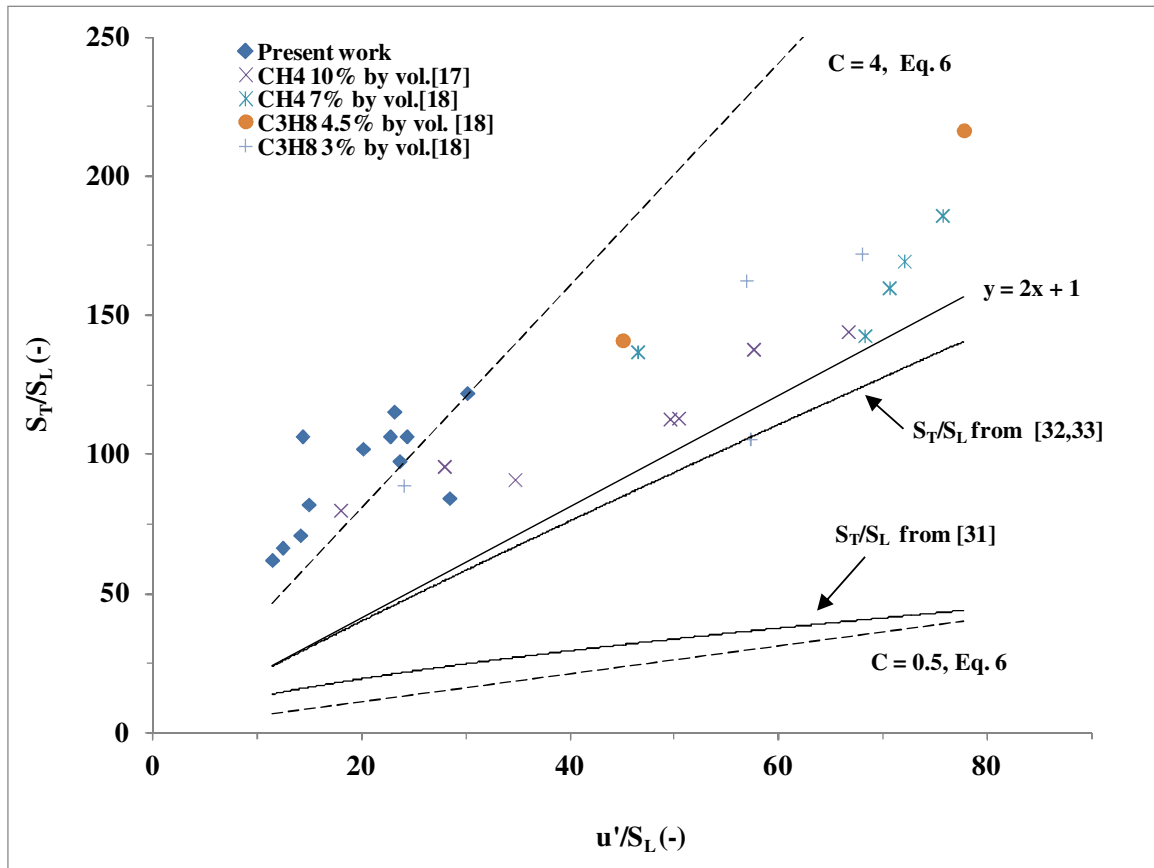


Fig. 8. Turbulent burning velocity as a function of the  $u'/S_L$ .

The present low-BR two-obstacle results for 10% methane/air in Fig. 8 lie close to the line with  $C = 4$  in Eq. 6 [33], but the previous results of Na'inna et al. with two interacting grid plates with 30% BR [17,18] were closer to  $C = 2$  at the higher  $u/S_L$  of this work.  $S_T/S_L$  ratios of 55 to 120 were found for two interacting bar type grid plates with a BR of 20%. The previous work of Na'inna et al. [17,18] for a BR of 30% with two single hole orifice baffles had a  $S_T/S_L$  from 60 to 220. Both of these sets of results show the turbulent enhancements necessary to explain the fast flames in unconfined vapour cloud explosions in the presence of obstacles. In incidents such as Flixborough, Buncefield and Texas City, overpressures were of the order of 1 bar. It may be shown that this requires a flame speed of about 300 m/s [15,16,20-22,32] and for a typical adiabatic hot gas expansion ratio of 8 this requires turbulent burning velocities of about 37 m/s and for a laminar burning velocity of 0.4 m/s this gives  $S_T/S_L$  of 92, which increases to around 200 if the mixture was very lean or rich rather than stoichiometric.

Phylaktou *et al.* [32] have shown that obstacles can increase flame speeds to over 1000 m/s if the upstream flow velocity is high enough. The present work deliberately investigated two interacting obstacles of low blockage ratio as single obstacles of high blockage have been shown to accelerate flames to over 600 m/s using the present test facility. Two obstacles of high blockage would accelerate to detonation and this has been observed on this test facility. However, two obstacles of low blockages but widely spaced is a low congestion scenario and it should be appreciated that this can be extremely dangerous for explosion acceleration.

#### 4. Conclusions

For single flat bar obstacles (1-4 flat bars), a dependence of the maximum overpressure and flame speed on the obstacle scale,  $b$  was shown to have  $P_{max}$  scaling with  $b^{0.33}$  and the flame speed scaling with  $b^{0.15}$ , and this agrees with a roughly square relationship between overpressure and flame speed.

An influence of obstacle spacing was apparent in terms of both the maximum pressure and the profile of the pressure development for double obstacle of similar blockage ratio, but different

obstacle separation distance. It was observed that the peak overpressure increased with the reduction in number of flat-bars, (that is increase in obstacle scale,  $b$ ). A maximum overpressure of 129 kPa was obtained for 1 flat-bar obstacles spaced at 2.25 m. For 2 flat-bar obstacles spaced at 1.25 m, a peak overpressure of 118 kPa was attained whereas 110kPa was realised for 4-flat-bar obstacles with obstacle separation distance of 0.5 m.

In order to widen the applicability of the present work, explosion test data were presented in terms of fundamental turbulent combustion parameters such as r.m.s velocity, turbulent velocity, turbulent Reynolds number and Karlovitz number. This allowed for comparison to other data and combustion models in the literature and thus widens the usefulness and applicability of the work. For all test conditions, a turbulent to laminar velocity ratio,  $S_T/S_L$  downstream of the obstacles of 62–122 indicating high turbulence level were attained. The average value of the  $S_T/S_L$  range (i.e.  $S_T/S_L$  of 92) is similar to that obtained from the analysis of some real gas explosion incidents such as Buncefield and Flixborough accidents. It is worth appreciating that with just two obstacles separated at optimum spacing, a higher explosion severity in terms of overpressure, flame speed and turbulence level similar to real gas explosion accidents could be realized.

## Acknowledgements

The authors are thankful to the Nigerian Petroleum Technology Development Fund (PTDF) Overseas Scholarship Scheme, for supporting Abdulmajid Na'inna in his PhD studies.

## References

1. J.H.S. Lee, I.O. Moen., "The mechanism of transition from deflagration to detonation in vapour cloud explosions," *Prog. in Energy and Combust. Sci.* 6 (4) (1980) 359-389.
2. ATEX (Explosive Atmosphere) 2014/34/EU, European Commission, 2014.

3. I.O. Moen, M. Donato, R. Knystautas, J.H. Lee., "Flame acceleration due to turbulence produced by obstacles," *Combust. Flame* 39 (1) (1980) 21-32.
4. I.O. Moen, J.H.S. Lee, B.H. Hjertager, K. Fuhre, R.K. Eckhoff., " Pressure development due to turbulent flame propagation in large-scale methane-air explosions," *Combust. Flame* 47 (0) (1982) 31-52.
5. A.J. Harrison, J.A. Eyre., " The effect of obstacle arrays on the combustion of large premixed gas/air clouds," *Combust. Sci. Technol.* 52 (1-3) (1987) 121-137.
6. G. Ciccarelli, C.J. Fowler, M. Bardon., " Effect of obstacle size and spacing on the initial stage of flame acceleration in a rough tube," *Shock Waves* 14 (3) (2005) 161-166.
7. A. Teodorczyk, P. Drobnik, A. Dabkowski., "Fast turbulent deflagration and DDT of hydrogen–air mixtures in small obstructed channel," *Intl. J. Hydrogen Energy* 34 (14) (2009) 5887-5893.
8. W. Rudy, R. Porowski, A. Teodorczyk., " Propagation of hydrogen-air detonation in tube with obstacles," *J. Power Technol.* 91 (3) (2011) 122-129.
9. R. Porowski, A. Teodorczyk., "Experimental study on DDT for hydrogen–methane–air mixtures in tube with obstacles," *J. Loss Prev. Process Ind.* 26 (2) (2013) 374-379.
10. L. Pang, Q. Zhang, T. Wang, D.C. Lin, L. Cheng, "Influence of laneway support spacing on methane/air explosion shock wave," *Safety Science*, 50(1) (2012) 83-89.
11. L.R. Boeck, J. Hasslberger, F. Ettner, T. Sattelmayer, Investigation of Peak Pressures during Explosive Combustion of Inhomogeneous Hydrogen-Air Mixtures, "*Proc. of the Seventh International Seminar on Fire & Explosion Hazards (ISFEH7)*, Providence, USA" 2013, p. 959–965.
12. G. Ma, J. Li, M. Abdel-jawed., "Accuracy improvement in evaluation of gas explosion overpressure in congestion with safety gaps," *J. Loss Prev. Process Ind.* 32 (2014) 358-366..
13. C. Wang, F. Huang, E. Kwasi Addai, X. Dong, "Effect of concentration and obstacles on flame velocity and overpressure of methane-air mixture" *J. Loss Prev. Process Ind.* 43 (2016) 302-310.

14. W.P.M. Mercx, D.M. Johnson, J. Puttock., "Validation of scaling techniques for experimental vapor cloud explosion investigations," *Process Saf. Prog.* 14 (2) (1995) 120-130.
15. C.L. Gardner, H.N. Phylaktou, G.E. Andrews, Turbulent Explosion Scaling: An assessment of experimental data., "Proc. of the Third International Seminar on Fire and Explosion Hazards (ISFEH3), Windermere, UK," 2000, p. 665-676.
16. H. Phylaktou, G.E. Andrews., " The acceleration of flame propagation in a tube by an obstacle," *Combust. Flame* 85 (3–4) (1991) 363-379.
17. A.M. Na'inna, H.N. Phylaktou, G.E. Andrews., "The acceleration of flames in tube explosions with two obstacles as a function of the obstacle separation distance," *J. Loss Prev. Process Ind.* 26 (6) (2013) 1597-1603.
18. A.M. Na'inna, H. Phylaktou, G.E. Andrews, Acceleration of flames in tube explosions with two obstacles as a function of the obstacle separation distance: the influence of mixture reactivity., " Proc. of the Seventh International Seminar on Fire and Explosion Hazards (ISFEH7), Providence, USA," 2013, p. 627-636.
19. A.M. Na'inna, H.N. Phylaktou, G.E. Andrews., " Effects of obstacle separation distance on gas explosions: the influence of obstacle blockage ratio," *Procedia Engineering* 84 ( 2014 ) 306 – 319.
20. H. Phylaktou, G.E. Andrews., " Application of turbulent combustion models to explosion scaling," *Process Saf. Env. Protect.* 73 (1) (1995) 3-10.
21. C.L. Gardner, H.N. Phylaktou, G.E. Andrews., "Turbulent Reynolds number and turbulent flame quenching influences on explosion severity with implications for explosion scaling," *ICChemE Symp.* 144 (1998) 279-292.
22. H.N. Phylaktou, Y. Liu, G.E. Andrews., " Turbulent explosions: a study of the influence of the obstacle scale," *ICChemE Symp.* 134 (1994) 269 - 284.
23. W.D. Baines, E.G. Peterson., "An investigation of flow through screens,"*Trans. ASME* 73 (1951) 167.

24. H.N. Phylaktou, G.E. Andrews., "Prediction of the maximum turbulence intensities generated by grid-plate obstacles in explosion-induced flows," *Symp. (Intnl.) Combust.* 25 (1) (1994) 103-110.
25. ISO 5167-2., "Measurement of fluid flow by means of pressure differential devices inserted in circular cross-section conduits running full - Part 2: Orifice plates," (2003).
26. A.J. Ward Smith, ed., "*Pressure losses in ducted flows*," Butterworths: London. 1971.
27. B. Karlovitz., "*Selected combustion problems*," Butterworths: London. 1954.
28. R.G. Abdel-Gayed, K.J. Al-Khishali, D. Bradley., "Turbulent burning velocities and flame straining in explosions" *Proc. R. Soc. Lond. A.* 391 (1801) (1984) 393-414.
29. R.G. Abdel-Gayed, D. Bradley., "Criteria for turbulent propagation limits of premixed flames," *Combust. Flame* 62 (1) (1985) 61-68.
30. R.G. Abdel-Gayed, D. Bradley, M. Lawes., "Turbulent burning velocities: a general correlation in terms of straining rates," *Proc. R. Soc. Lond, A.* 414 (1847) (1987) 389-413.
31. D. Bradley, A.K.C. Lau, M. Lawes., " Flame stretch rate as a determinant of turbulent burning velocity," *Proc. R. Soc. Lond, A.* 338 (1650) (1992) 359-387.
32. H.N. Phylaktou, A. Alexiou, G.E. Andrews., "Interactions of fast explosions with an obstacle," *Report No. OTI 94 625, HSE, Offshore Technology* 1995.
33. H.N. Phylaktou, G.E. Andrews, N. Mounter, K.M. Khamis., "Spherical explosions aggravated by obstacles," *IChemE Symp.* 130 (1992) 526.